Structural Transformations and Defect Production in Ion Implanted Silicon: A Molecular Dynamics Simulation Study

T. Diaz de la Rubia
Lawrence Livermore National Laboratory, L-268, P.O. Box 808, Livermore, California 94550

G. H. Gilmer
AT&T Bell Laboratories, Room 1E-332, 600 Mountain Avenue, Murray Hill, New Jersey 07974
(Received 8 September 1994)

We have simulated collisions of 5 keV silicon atoms with a silicon substrate. At this energy the simulation provides an atomistic description of the evolution of the displacement cascade. We discuss the structural changes occurring as the cascade regions transform from crystalline to liquid to amorphous phases. We compare the structure of the amorphous material with that of rapidly quenched liquid silicon. We also discuss the time evolution of the stress, kinetic and potential energies, and atomic density. An assessment of defect production mechanisms is made.

PACS numbers: 61.80.Az

Low energy ions are used extensively in the manufacturing of semiconductor devices [1]. Implantation of dopant atoms, smoothing and cleaning of surfaces, and metallization are all processes that can involve collisions of energetic ions and atoms with crystalline material. The manufacturing of ever smaller feature size semiconductor devices requires precise control of the dopant distribution following ion implantation and rapid thermal annealing. The defects and strain produced by the implantation of dopant ions can have dramatic effects on the diffusion of dopant atoms, but the mechanisms are not completely understood at present [2]. Therefore, understanding the atomistic nature of the damage produced by low energy (keV) collision cascades in silicon has become an issue of critical importance.

Large doses of ions can also produce an amorphous layer parallel to the substrate surface. Several models have been proposed to describe the transition from local damage regions resulting from individual ion cascades to a continuous layer [3]. There is experimental evidence that the volume fraction of amorphous material increases in a superlinear way with dose, resulting in an abrupt transition to a layer with flat amorphous/crystal interfaces [4,5]. This suggests that more amorphous material is created when ions collide with material which has already been subjected to a small amount of ion-induced damage. Such a result could be explained if the amorphous pockets produce stress fields which increase in magnitude with dose, or if there were an accumulation of mobile defects which tend to destabilize the lattice. Atomistic simulations have sufficient detail to treat these aspects of ion implantation.

Molecular dynamics (MD) simulations have been used to study sputtering and defect production in silicon using ion energies in the range of 1 keV and below. Some of the details of the collisions including the formation of shock waves and the early stages of damage formation have been reported [6,7]. In this Letter we have employed primary knock-on atom (PKA) energies of 5 keV which is characteristic of the range of energies being used to implant dopants for shallow junctions in semiconductor devices [1].

We describe the results of several 5 keV collisions, and provide data on the evolution of structure in the cascade regions, the atomic-level stress, the kinetic energy E_K, and the density. We also discuss the production and structure of pockets of disordered material and their relation to the production of Frenkel defects. Precise information on the point defects and lattice disorder produced by implantation and on the effect of annealing the region of the implant could provide useful data for finite element models of semiconductor device processing [8].

Results from a typical simulation are illustrated in Fig. 1. The computational cell is illustrated by the black lines, and the base of the cell is a square 152 Å on an edge, and the height is 135 Å. There are 160 000 silicon atoms in the cell, and at the start of the simulations they occupy perfect diamond cubic lattice sites. A (001) crystal-vacuum interface is at the top, and an atom at the center of the top (001) layer is given an initial velocity corresponding to a kinetic energy of 5 keV, as illustrated by the red line. This atom will be referred to as the PKA. The Stillinger-Weber potential is used to calculate forces between atoms [9]. The atoms in the layer at the bottom of the computational cell are held fixed in their initial positions, and all other atoms are allowed to move according to the forces exerted by their neighbors using classical molecular dynamics techniques [10]. The atoms in the two layers above the bottom layer and the outermost two atom planes in the (100) and (010) directions are coupled to a heat bath via the Langevin equation of motion to maintain a constant temperature. Periodic boundary conditions are applied along (100) and (010).

0031-9007/95/74(13)/2507(4)$06.00

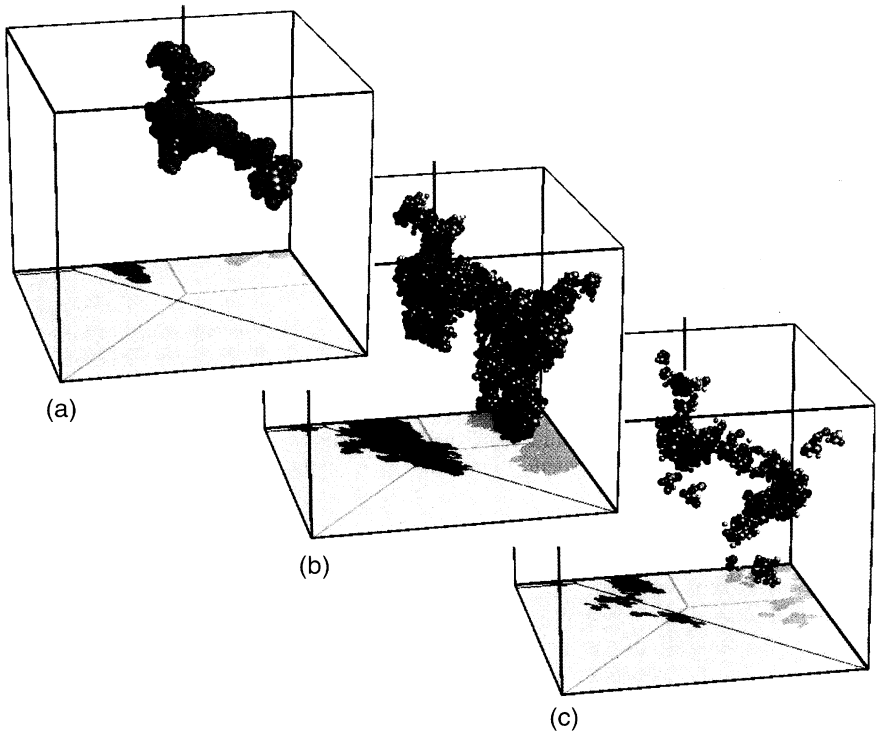

FIG. 1. Configurations of atoms with potential energy greater than 0.2 eV above the crystal ground state value. Sphere size indicates energy of the atoms from 0.2 to 1 eV and above. Color represents atomic-level stress with blue indicating tensile stress and red indicating compressive stress. The development of damage with time is indicated in the sequence; (a) corresponds to 0.1 ps after the ion starts moving, (b) to 1 ps, and (c) to 8 ps.

The region damaged by a typical 5 keV ion is shown in the snapshots of Fig. 1. Only atoms with potential energies E_P of 0.2 eV above the ground state are illustrated. The diameter provides an indication of atom potential energies above 0.2 eV, with the maximum size corresponding to atoms above 1 eV. The color of the spheres indicates atomic-level stress σ, where $\sigma = \Omega^{-1}\partial V(\zeta r_{ij})/\partial\zeta$, and Ω is the atomic volume of the crystal, and ζ is a distance scaling factor. The color scale ranges from blue for tensile stress to red for compressive stress. The initial substrate temperature was 80 K in this case.

At the start of the collision process, the energy is concentrated in a relatively small number of atoms with large potential energies, as shown in Fig. 1(a). At this time, 0.1 ps after the start of the 5 keV atom, the region of damage has not extended to its full depth, and the cascade region is under large compressive stress. The maximum number of atoms with $E_P > 0.2$ eV occurs about 0.2 ps after the first collision; at this point the average total energy per atom is $\approx$1 eV for those atoms with $E_P > 0.2$ eV. The average potential energy of the particles illustrated in Fig. 1(b) ($t = 1$ ps) is 0.47 eV, whereas the latent heat of fusion of the silicon model is 0.325 eV, suggesting that these particles may have properties similar to that of liquid silicon. Figure 1(c) shows that about 5×10^2 atoms still have $E_P \geq 0.2$ eV after 8 ps; the average potential energy of these atoms is 0.34 eV.

The structure of the material in a cascade region changes dramatically during the period of the simulation. Figure 2 shows the radial distribution function (rdf) at two different times for a region in the core of the cascade at 1 ps [cf. Fig. 1(b)]. The structure shown in Fig. 2(a), corresponding to 1.1 ps, is similar to that of bulk liquid silicon at the melting point, Fig. 2(c), although the peaks are broadened and less distinct in the case of the cascade. The final structure at 7 ps, Fig. 2(b), is similar to that obtained for the bulk amorphous Stillinger-Weber modeled (SW) silicon, in the case were the liquid is cooled from the melting point to 0 K in 5 ps, Fig. 2(d). Note the presence in both cases of a peak at 3.4 Å, corresponding to the shoulder that is usually observed for amorphous SW silicon at finite temperatures [11–13]. In Fig. 2(e) we show the rdf for a quench 2 orders of magnitude slower, i.e., in 500 ps [14]. The rdf from the slower quench exhibits a peak at 3.4 Å that is much reduced in height. This comparison with the structure of the quenched liquid indicates that the amorphous material in this region has a structure that is determined

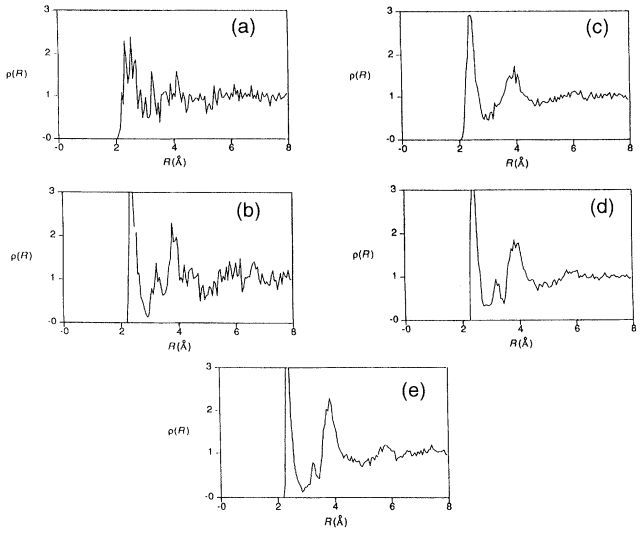

FIG. 2. The radial distribution function (rdf) of atoms in a cascade region [(a) corresponds to 1.1 ps and (b) to 8 ps] are compared with those of bulk silicon. (c) is the rdf for liquid silicon at the melting point, (d) is the rdf for amorphous silicon quenched from the melt in 5 ps, and (e) is the rdf from amorphous silicon quenched from the melt in 500 ps.

by the fast quench of the liquidlike cascade region by the conduction of heat to the surrounding crystal. The average coordination number in this region, as determined from the integral of $g(r)$ out to the first minimum, was found to increase to a value of $\approx$6.5 at 0.5 ps and decrease to $\approx$4.3 after equilibration with the surrounding lattice. Similarly, the density in the region initially decreases to a value 10% smaller than the crystalline density and then changes to a value slightly larger ($\approx$3%) than the equilibrium density at $\approx$0.5 ps. At early times, due to the energetic collisions the average atomic stress increases to a compressive value of 10^{12} dyn/cm^2, and then changes sign to tensile stress at about 0.5 ps, consistent with the density and coordination number changes described above.

The results of these MD simulations provide insight into the defect production process in silicon. One of the most striking results of this work is the fact that very few isolated Frenkel pairs are produced directly by the displacement cascades. This can be understood by considering that isolated point defects are produced in cascades by replacement collision sequences (RCS's) along low index crystallographic directions [15,16]. As we have recently shown, such RCS's in silicon are extremely short, 2 to 3 atomic replacements long at most [17]. Therefore, the probability of such an RCS producing a stable (i.e., separated beyond its own spontaneous recombination volume) vacancy-interstitial pair during a keV cascade is very small. On the other hand, large pockets of unrelaxed amorphous material are produced by the displacement cascades. For these 5 keV cascades, the disordered regions contain an average of $\approx$800 atoms, i.e., 7 times the number predicted by binary collision approximation calculations [18]. Because of the energetic collisions and the density changes induced by the incoming particle, these amorphous regions frequently have densities that differ from that of the crystal. Also, because of their large surface-to-volume ratio and the fact that they are surrounded by crystalline material, these amorphous pockets are highly unstable, and recrystallize at much lower temperatures than a stable planar amorphous/crystal interface. Upon annealing for several picoseconds at elevated temperature, such density fluctuations result in the appearance of vacancies and self-interstitial atoms in the recrystallized material. This process is illustrated in Fig. 3. In Fig. 3(a), we select a small region of the crystal where amorphous material has been produced as a result of a 5 keV cascade. Upon annealing for 1 ns at 1300 K, Fig. 3(b) shows that the amorphous material has recrystallized and a distribution of monovacancies (1), vacancy clusters (2 divacancies and 1 tri-vacancy), and $\langle 110 \rangle$ dumbbell self-interstitials (3) is present. These defects can then participate in the transient enhanced diffusion of dopant atoms that is commonly observed in low energy ion implanted silicon. Note that out of approximately 500 atoms originally present in the annealed amorphous pocket, only 2 new self-interstitials, one monovacancy, two divacancies, and a trivacancy remain as damage.

These results help explain many experimental observations of intrinsic dislocation (interstitial type) loop growth during the annealing of silicon following implantation. Schreutelkamp *et al.* [19] have shown that implantation with low energy ions in silicon can result in dislocation loop formation during subsequent annealing at 900 °C if the number of displaced atoms exceeds a critical value. However, their RBS-channeling measurements showed that for 100 keV irradiation of silicon with P^+, only about 0.07% of displaced atoms end up in the loops. This is consistent with our observation that displacement cascades produce large amorphous pockets and few isolated, freely migrating defects. As we have shown above, when the amorphous pockets recrystallize during annealing, point defects and defect clusters appear in the lattice. Nevertheless, their number is only a small fraction, approximately 1% or less, of the number of atoms originally present in the amorphous pockets.

In conclusion, we have simulated the collisions of 5 keV silicon ions with a silicon substrate. We find that amorphous material is left after the cascades cool to the ambient temperature. The average number of atoms in the amorphous regions is about 800, in agreement with the 10 eV/atom amorphization energy observed in ion implantation experiments on a number of different systems [20]. The structure of the amorphous regions

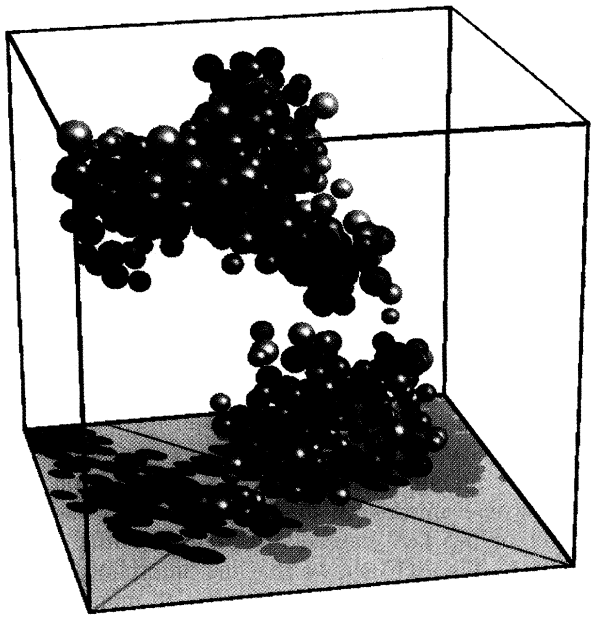

(a)

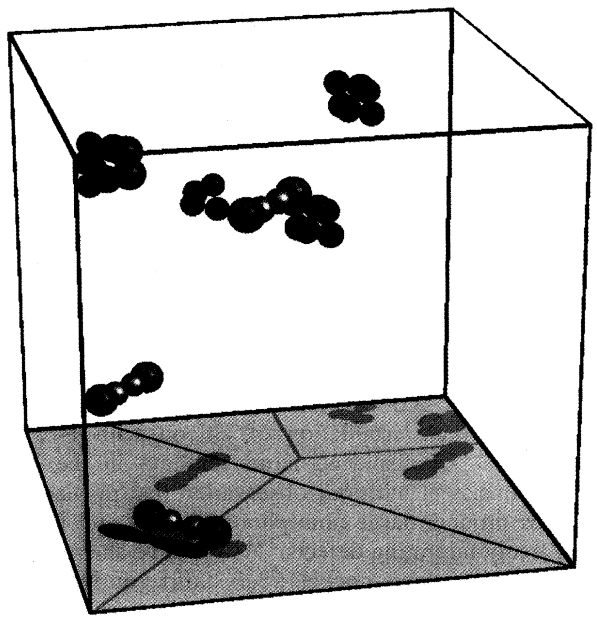

(b)

FIG. 3. Annealing of cascade-induced amorphous pockets by molecular dynamics. (a) State immediately after the cascade. (b) After 1 ns annealing at 1300 K the amorphous material has recrystallized and self-interstitials and vacancy clusters are left behind. The vacancies and their clusters induce tensile stress in the neighboring atoms and these are shown as blue spheres. The self-interstitials are shown as red and gray spheres.

is similar to that of bulk silicon quenched from the melting point to 0 K in 5 ps. This is consistent with the fact that the cascade regions have a structure similar to liquid silicon during the approximately 2 ps period that the kinetic energy in the region is close to that of liquid silicon. Tensile stress results from the collisions, and the density of the silicon substrate in increased. Finally, the 5 keV PKA's produce few if any isolated Frenkel pairs. However, the amorphous regions contain several hundred displaced atoms. These regions often contain a deficit or an excess of atoms when compared with the perfect crystal, and simulations of annealing for several picoseconds at high temperatures can cause these regions to collapse into clusters of interstitials or vacancies. We expect that these defect clusters are primarily responsible for the enhanced diffusion of dopant atoms commonly observed in low energy ion implanted silicon.

The authors have benefited from extensive discussions with J. M. Poate, R. S. Averback, M. W. Guinan, and C. A. Volkert. Work by T. Diaz de la Rubia was performed under the auspices of the U.S. Department of Energy by Lawerence Livermore National Laboratory under Contract No. W-7405-Eng-48.

[1] *Handbook of Ion Implantation Technology,* edited by J. F. Ziegler (North-Holland, Amsterdam, 1992).
[2] P. M. Fahey, P. B. Griffin, and J. D. Plummer, Rev. Mod. Phys. **61**, 289 (1989).
[3] For a recent review, see, e.g., S. U. Campisano, S. Coffa, V. Raineri, F. Priolo, and E. Rimini, Nucl. Instrum. Methods Phys. Res., Sect. B **80/81**, 514 (1993).
[4] O. W. Holland, S. J. Pennycook, and G. L. Albert, Appl. Phys. Lett. **55**, 2503 (1989).
[5] G. Bai and M.-A. Nicolet, J. Appl. Phys. **70**, 649 (1991).
[6] D. Stock *et al.,* Rad. Eff. Def. Solids **130**, 67 (1994).
[7] R. Smith, D. E. Harrison, Jr., and B. J. Garrison, Phys. Rev. B **40**, 93 (1989).
[8] D. A. Antoniadis and R. W. Dutton, IEEE J. Solid-State Circuits **14**, 412 (1986).
[9] F. H. Stillinger and T. A. Weber, Phys. Rev. B **31**, 5262 (1985).
[10] M. P. Allen and D. J. Tildesley, *Computer Simulation of Liquids* (Oxford University Press, Oxford, 1987).
[11] J. Q. Broughton and X.-P. Li, Phys. Rev. B **35**, 9120 (1987).
[12] W. D. Luedtke and U. Landman, Phys. Rev. B **37**, 4656 (1988).
[13] I. Kwon *et al.,* Phys. Rev. B **41**, 3678 (1990).
[14] G. H. Gilmer and T. Diaz de la Rubia (unpublished).
[15] J. B. Gibson *et al.,* Phys. Rev. **120**, 1229 (1960).
[16] T. Diaz de la Rubia, R. S. Averback, R. Benedek, and W. E. King, Phys. Rev. Lett. **59**, 1930 (1987).
[17] M.-J. Caturla, T. Diaz de la Rubia, and G. H. Gilmer, Mater. Res. Soc. Symp. Proc. **316**, 141 (1994).
[18] P. Sigmund, Rad. Eff. **1**, 15 (1969).
[19] R. J. Schreutelkamp *et al.,* Mater. Sci. Rep. **6**, 275 (1991).
[20] W. L. Brown and A. Ourmazd, MRS Bull. **17**, 30 (1992).

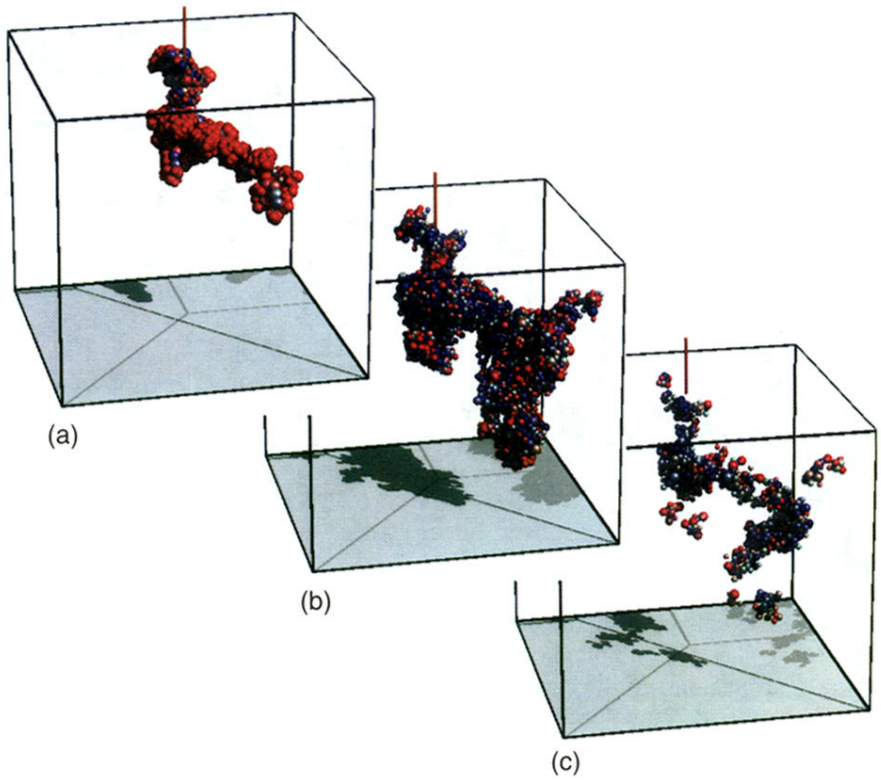

FIG. 1. Configurations of atoms with potential energy greater than 0.2 eV above the crystal ground state value. Sphere size indicates energy of the atoms from 0.2 to 1 eV and above. Color represents atomic-level stress with blue indicating tensile stress and red indicating compressive stress. The development of damage with time is indicated in the sequence; (a) corresponds to 0.1 ps after the ion starts moving, (b) to 1 ps, and (c) to 8 ps.

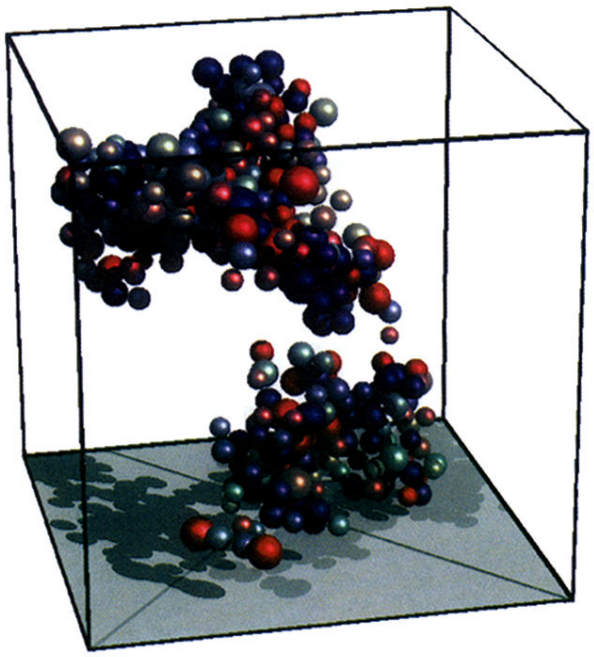

(a)

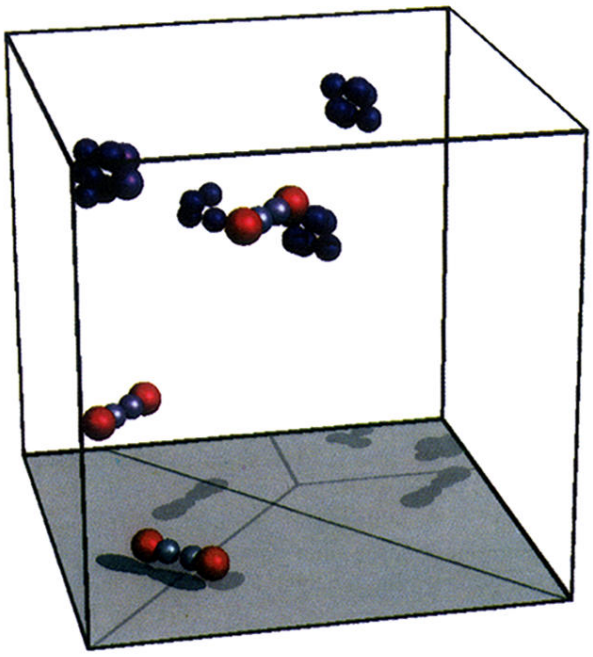

(b)

FIG. 3. Annealing of cascade-induced amorphous pockets by molecular dynamics. (a) State immediately after the cascade. (b) After 1 ns annealing at 1300 K the amorphous material has recrystallized and self-interstitials and vacancy clusters are left behind. The vacancies and their clusters induce tensile stress in the neighboring atoms and these are shown as blue spheres. The self-interstitials are shown as red and gray spheres.